




Overview of Impaired BDNF Signaling, Their Coupled Downstream Serine-Threonine Kinases and SNARE/SM Complex in the Neuromuscular Junction of the Amyotrophic Lateral Sclerosis Model SOD1-G93A Mice

Laia Just-Borràs¹ · Erica Hurtado¹ · Víctor Cilleros-Mañé¹ · Olivier Biondi² · Frédéric Charbonnier² · Marta Tomàs¹ · Neus Garcia¹ · Maria A. Lanuza¹  · Josep Tomàs¹

Received: 14 December 2018 / Accepted: 13 March 2019 / Published online: 30 March 2019
© Springer Science+Business Media, LLC, part of Springer Nature 2019

Abstract

Amyotrophic lateral sclerosis (ALS) is a chronic neurodegenerative disease characterized by progressive motor weakness. It is accepted that it is caused by motoneuron degeneration leading to a decrease in muscle stimulation. However, ALS is being redefined as a distal axonopathy, in that neuromuscular junction dysfunction precedes and may even influence motoneuron loss. In this synapse, several metabotropic receptor-mediated signaling pathways converge on effector kinases that phosphorylate targets that are crucial for synaptic stability and neurotransmission quality. We have previously shown that, in physiological conditions, nerve-induced muscle contraction regulates the brain-derived neurotrophic factor/tropomyosin-related kinase B (BDNF/TrkB) signaling to retrogradely modulate presynaptic protein kinases PKC and PKA, which are directly involved in the modulation of acetylcholine release. In ALS patients, the alteration of this signaling may significantly contribute to a motor impairment. Here, we investigate whether BDNF/TrkB signaling, the downstream PKC (cPKC β I, cPKC α , and nPKC ϵ isoforms), and PKA (regulatory and catalytic subunits) and some SNARE/SM exocytotic machinery proteins (Munc18-1 and SNAP-25) are altered in the skeletal muscle of pre- and symptomatic SOD1-G93A mice. We found that this pathway is strongly affected in symptomatic ALS mice muscles including an unbalance between (I) BDNF and TrkB isoforms, (II) PKC isoforms and PKA subunits, and (III) Munc18-1 and SNAP-25 phosphorylation ratios. Changes in TrkB.T1 and cPKC β I are precociously observed in presymptomatic mice. Altogether, several of these molecular alterations can be partly associated with the known fast-to-slow motor unit transition during the disease process but others can be related with the initial disease pathogenesis.

Keywords ALS · TrkB · PKC · PKA · BDNF · Munc18-1 · SNAP-25 · Skeletal muscle · NMJ

Introduction

Amyotrophic lateral sclerosis (ALS) is a chronic neurodegenerative disease characterized by progressive motor weakness and loss of muscle innervation originating from selective motoneuron (MN) cell death. Consequently, it causes synaptic dysfunction at the neuromuscular junction (NMJ) as well as in other synapses [1, 2]. Although several cellular processes are altered in ALS patients and mouse models, including glutamatergic excitotoxicity and oxidative stress, the precise pathogenesis of the disease remains unknown. About 90% of ALS cases are sporadic, and only the 10% of the cases are familial (FALS) [3]. Genetic studies in FALS patients have

L. Just-Borràs, E. Hurtado, M. A. Lanuza, N. Garcia and J. Tomas contributed equally to this work.

✉ Maria A. Lanuza
mariaangel.lanuza@urv.cat

✉ Josep Tomàs
josepmaria.tomas@urv.cat

¹ Unitat d'Histologia i Neurobiologia (UHNEUROB), Facultat de Medicina i Ciències de la Salut, Universitat Rovira i Virgili, Carrer St Lorenc num 21, 43201 Reus, Spain

² INSERM UMRS 1124 and Université Paris Descartes, 45 rue des Saints-Pères, 75270 Paris Cedex 06, France

identified different mutations in genes including ataxin-2, TDP-43, Fus, and C9ORF72 [4]. However, about the 20% of the cases can be attributed to a mutation-induced misfolding in the $\text{Cu}^{2+}/\text{Zn}^{2+}$ superoxide dismutase 1 (SOD1), which is a ubiquitously expressed free-radical defense enzyme [5, 6]. Because of that, the overexpression of human mutant SOD1 in transgenic mice, which mimics the symptoms and progression of the human disease, has been extensively used to study ALS pathophysiology.

It is widely accepted that ALS is caused by MN degeneration. However, it has been shown that NMJ degeneration appears before the pathology shows up in animal models [7] and in humans [8]. Because the loss of the correct contact between MN and muscle cells contributes to motor impairment (atrophy and paralysis) in different diseases, the NMJ alteration could be a primary cause for ALS. In this context, many mechanisms explaining the early NMJ alteration have been proposed such as the disruption of anterograde/retrograde axonal transport, genomic and proteomic changes and abnormal cellular metabolism and/or tropism of the cells making synapse [9, 10].

The brain-derived neurotrophic factor/tropomyosin-related kinase B (BDNF/TrkB) neurotrophic signaling is one of the most implicated in the maintenance of synapses and the neuronal survival in the CNS, and it is also implicated in NMJ stability and functionality [11–15]. Indeed, several studies have demonstrated that BDNF prevents lesion-induced degeneration of spinal motoneurons in neurodegenerative disease models [16–19]. Genetic manipulation of p75^{NTR} , a member of the tumor necrosis factor receptor family, and BDNF/TrkB signaling is effective in the treatment of ALS in animal models [20, 21]. Moreover, TrkB.T1 deletion significantly slows the onset of motoneuron degeneration in an ALS mice model [22] while the functional isoform of TrkB receptor (TrkB.F1) is much less phosphorylated in ALS spinal cords [23], indicating that it is less functional in the pathology. However, despite these evidences, all preclinical [24] and clinical [25] attempts to modulate the BDNF/TrkB signaling in the CNS failed to demonstrate beneficial effects on motor neuron survival [26, 27], indicating that further investigation on this signaling pathway is needed. Neuromuscular activity is an essential regulator of BDNF/TrkB signaling in the skeletal muscle, which triggers the activity of presynaptic PKC isoforms (cPKC β I and nPKC ϵ) to adapt neurotransmission through the phosphorylation of key molecules of the synaptic vesicle exocytosis, such as the SM protein Munc18-1 and the SNARE protein SNAP-25 [14, 28–30]. However, no information about how the BDNF/TrkB signaling is affected in the skeletal ALS muscle and which role this signaling could play on the primary degeneration of the NMJ has been reported.

Fast-twitching muscles are more affected by ALS than slow-twitching muscles, due their functional properties [31]. Moreover, during ALS progression, fast-twitch muscles undergo a fast-to-slow transition [32, 33] because surviving slow motor neurons sprout over denervated fast-twitch myofibers

in an activity-dependent way [33]. Furthermore, extra-ocular muscles, which are known to be the fastest muscles in mammals, are far less affected than limb and respiratory muscles [34, 35], due to their specific characteristics [31, 36].

All these data evidence that there could be a relation between the activity-dependent BDNF/TrkB/PKC signaling in the muscle and ALS phenotype, suggesting that its alteration could contribute to a deficient regulation of the presynaptic function. This could decrease the synaptic protection capability and affect the retrograde neuroprotection over the MNs. Because of that, our aim is to investigate how this pathway is (1) affected in the fast-twitch plantaris of pre- and symptomatic ALS mouse model, and (2) differentially expressed in control condition between the ALS-sensitive fast-twitch plantaris and the ALS-resistant slow-twitch soleus. This work will allow us (1) to evaluate how this pathway is altered in an ALS-involved fast-twitch muscle and (2) to link BDNF/TrkB signaling to muscle susceptibility to ALS.

Our results show, firstly, that the full BDNF/TrkB signaling is altered in symptomatic ALS plantaris and that some of the changes (i.e., TrkB.T1 isoform) appear precociously altered in presymptomatic muscles. Secondly, BDNF/TrkB signaling molecular pattern differs between control fast- and slow-twitch muscles, reinforcing their potentially protective role against the ALS-induced neuromuscular denervation. Moreover, we demonstrate that the alterations found in ALS plantaris can be partly explained by the well-known fast-to-slow transition during the disease process, but also by a specific ALS-dependent process, revealed by the increase of mature BDNF and TrkB.T1 levels, which could directly impact the pathogenesis.

Materials and Methods

SOD1-G93A Mice Model

Transgenic male B6/SJL-Tg (SOD1-G93A) 1Gur/J (Stock No. 002726) [37, 38] mice were purchased from The Jackson Laboratory (Bar Harbor, ME, USA). They were crossed with wild-type B6/SJL females (Janvier, Le Genest-Saint-Isle, France) and only littermate males were used in this study. This was done (i) to reduce variability in the results and (ii) because the incidence and prevalence of ALS are greater in men than in women [39]. All mice were kept on the animal facility under standard conditions: constant temperature (22 ± 2 °C), relative humidity ($50 \pm 10\%$) and a 12-h light/dark schedule. All experimental procedures, which included minimizing the number of animals used and their suffering, were approved by the policies of the French Agriculture and Forestry Ministry and by the Animal Research Committee of the Universitat Rovira i Virgili following the guidelines of the EU Directive 2010/63/EU for animal experiments.

ALS onset was defined as the time corresponding to the first observation of myotonia symptoms in the mice hind limb

(around P90) and the disease progression was assessed by a trained observer that evaluated myotonia symptoms and weighing. Five animals were euthanized at P50 (ALS P50), which represents a presymptomatic stage of the disease and five animals at P115 (ALS P115), which represents the end stage of the disease. Five littermates of these animals without the mutation were used as controls (WT P50 and WT P115).

Antibodies

Primary and secondary antibodies used for Western blot and immunohistochemistry (described below) analysis were obtained from different commercial manufacturers and are specified in Table 1. As a control, primary antibodies were omitted from some samples. These controls never revealed bands of

the appropriate molecular weight nor staining in nonspecific regions. All antibodies specificity has been previously determined [14, 28, 30, 40, 41].

Western Blotting

Mice muscles were dissected and frozen in liquid nitrogen and homogenized using a manual homogenizer in ice-cold lysis buffer (in mM: NaCl 150, Tris-HCl (pH 7.4) 50, EDTA 1, NaF 50, PMSF 1, sodium orthovanadate 1; NP-40 1%, Triton X-100 0.1%, and protease inhibitor cocktail 1% (Sigma-Aldrich, Saint Louis, MO, USA). Protein lysates were obtained collecting supernatants after removing insoluble materials by centrifugation at 4 °C and aliquots were stored at –80 °C.

Table 1 List of primary and secondary antibodies used

Target	Immunogen	Source	Reference	Dilution
BDNF	Peptide corresponding to the amino acids 130–247 of the human protein.	Rb pAb	Sc-20981	1/500
NT4	Peptide corresponding to an intern region of the human protein.	Rb pAb	Sc-545	1/500
p75 ^{NTR}	Peptide corresponding to the amino acids 274–425 of the rat protein.	Rb pAb	07-476	1/800
TrkB	Peptide corresponding to the amino acids 37–75 of the human protein.	Ms mAb	Sc-377218	1/1000
pTrkB (Tyr816)	Phosphopeptide corresponding to the sequence containing the Tyr816 near the C-terminus of the rat protein.	Rb pAb	ABN1381	1/1000
PKD1	Peptide corresponding to the amino acids 229–556 of the human protein.	Ms mAb	Sc-17765	1/1000
pDPK1 (Ser241)	Phosphopeptide corresponding to residues around Ser241 of the human protein.	Rb pAb	#3061	1/1000
cPKC α	Peptide corresponding to the C-terminus of the human protein.	Rb pAb	Sc-208	1/800
pcPKC α (Ser657)	Phosphopeptide corresponding to the amino acids 654–663 of the protein.	Rb pAb	06-822	1/1000
cPKC β I	Peptide corresponding to the C-terminus of the human protein.	Rb pAb	Sc-209	1/1000
pcPKC β I (Thr642)	Phosphopeptide corresponding to the residues around the phosphorylation site of Thr642.	Rb pAb	Ab75657	1/1000
nPKC ϵ	Peptide sequence corresponding to the C-terminus of the human protein.	Rb pAb	Sc-214	1/1000
pnPKC ϵ (Ser729)	Phosphopeptide sequence corresponding to the amino acids around the Ser729 of the human protein.	Rb pAb	Sc-12355	1/1000
PKA C α	Peptide corresponding to the C-terminus of the human protein.	Rb pAb	Sc-903	1/1000
PKA C β	Peptide corresponding to the C-terminus of the human protein.	Rb pAb	Sc-904	1/1000
PKA RI α	Peptide corresponding to the amino acids 1–381 (full sequence) of the human protein.	Ms mAb	Sc-136231	1/1000
PKA RI β	Peptide corresponding to the C-terminus of the human protein.	Rb pAb	Sc-907	1/1000
PKA RII α	Peptide corresponding to the C-terminus of the mouse protein.	Rb pAb	Sc-909	1/1000
PKA RII β	Peptide corresponding to the amino acids 21–110 mapping near the N-terminus of the human protein.	Ms mAb	Sc-376778	1/1000
Munc18-1	Peptide corresponding to residues around Tyr157 of human protein.	Rb mAb	13,414	1/1000
pMunc18-1 (Ser313)	Phosphopeptide corresponding to amino acids 307–319 (internal sequence) containing the Ser313 of the human protein.	Rb pAb	Ab138687	1/1000
SNAP-25	Peptide corresponding to residues surrounding Gln116 of human protein.	Rb mAb	#5309	1/1000
pSNAP-25 (Ser187)	Phosphopeptide corresponding to amino acids around Ser187 of the rat protein.	Rb pAb	Ab169871	1/1000
pSNAP-25 (Thr138)	Phosphopeptide corresponding to residues around Thr138 from the human protein.	Rb pAb	Orb163730	1/1000
ChAT	Human placental enzyme (full sequence)	Gt pAb	AB144	1/800
Secondary antibodies	Anti-rabbit conjugated HRP	Dk pAb	711-035-152	1/10,000
	Anti-mouse conjugated HRP	Rb pAb	A9044	1/10,000
	Anti-goat conjugated Alexa fluor 568	Dk pAb	A-11057	1/500

Protein concentrations were determined by DC protein assay (Bio-Rad, Hercules, CA, IL).

Protein samples of 30 µg were separated by 8 or 12% SDS-polyacrylamide electrophoresis and electrotransferred to a polyvinylidene difluoride (PVDF) membrane (Hybond™-P; Amersham, GE Healthcare) using Trans-Blot Turbo Transfer System (Bio-Rad, Hercules, CA). For immunodetection, membranes were blocked with Tris-buffered saline 0.1% Tween 20 (TBST) containing 5% (W/V) phosphoblocker or Bovine Serum Albumin (BSA) for phosphorylated proteins and non-fat dry milk for non-phosphorylated proteins for an hour. Then, membranes were incubated in primary antibody (Table 1) overnight and with a corresponding secondary antibody horseradish peroxidase conjugated for 1 h. Membranes were revealed with Bio-Rad ECL kid on the ChemiDoc XRS+ machine (Bio-Rad, Hercules, CA). The bands optical density was normalized in relation to (1) the background values and to (2) the total protein transferred on PVDF membranes, measured by total protein analysis (Sypro Ruby protein blot stain, Bio-Rad [42]).

The relative variations between ALS and WT plantaris were calculated from the same membrane image, and the same was done for soleus and tibialis WT muscles. Data was taken from densitometry measurements made in at least three separate western blots for each of the five animals in each group. To simplify data expression, the normalized value of the bands representing the control (both P115 and P50) animals was adjusted to 1 and the bands representing ALS animals were calculated in relation with the respective control ones.

Immunohistochemistry

The spinal cord of P115 mice ($n = 5$ in each group) was dissected after the animals were anesthetized by intraperitoneal injection of 3.5% chloral hydrate and perfused transcardially with buffered saline and 4% paraformaldehyde. Then, they were post-fixed in 4% PFA and rinsed two times in PBS azide 0.01% buffer. The L1 to L5 lumbar region of the spinal cord was sectioned with a vibrating blade microtome (VT-1000S, Leica Microsystems SAS, Nanterre, France) at 50 µm thickness. One out of every six sections was subsequently processed for immunostaining on free-floating sections (an average of seven sections per animal were studied). The immunohistochemical analysis was based on detection of choline acetyltransferase (ChAT) to stain motoneurons (Table 1). Moreover, DAPI was also used to stain cell nuclei. Sections were mounted in Vectashield mounting medium (Vector Laboratories, Burlingame, CA, USA) and collected with a CMOS camera (ORCA Flash 2.8, Hamamatsu Photonics France, Massy, France) mounted on a Zeiss AxioObserver microscope (Z1, Carl Zeiss SAS, Le Pecq, France) using the ZEN 2012 software (Carl Zeiss SAS). The staining specificity was checked by performing the incubation in the absence of the primary antibodies. All counts were performed using the ZEN 2012 software (Carl Zeiss SAS).

Statistical Analysis

All values are expressed as means ± standard deviation (SD) within each group. Statistical significance of the differences between WT and ALS groups was evaluated under a non-parametric Kruskal-Wallis test followed by Dunn's post hoc test. On the other hand, statistical significance of the differences between WT muscles was evaluated using the Friedman test and Bonferroni correction (Graph Pad Prism Software, San Diego, USA). All the data presented in this study were considered statistically different when the statistical power exceeds 95%. The criterion for statistical significance was: * $p < 0.05$, ** $p < 0.01$, and *** $p < 0.001$.

Results

Firstly, we analyzed total and phosphorylated protein levels of representative molecules of the BDNF-operated transmitter release regulation in the fast plantaris muscle (one of the most affected in ALS) of presymptomatic (50 days old) and symptomatic (115 days old) ALS mice. The entire neurotrophic pathway has been studied to its three molecular levels: (i) the neurotrophins BDNF and NT4 and their receptors TrkB and p75^{NTR}, (ii) the coupled serine-threonine kinases (PKC isoforms) and priming kinase—PDK1—and the different subunits of the cAMP-dependent kinase (PKA), and (iii) PKC and PKA targets related with neurotransmitter release. In addition to the figures showing quantitative data (Figs. 1, 2, 3, and 4), Fig. 6a (changes in P50), b (1) (P115) shows a schematic representation of the main results.

Neurotrophins and Receptors

To investigate how the BDNF signaling is affected in ALS mice, we compared mature BDNF (mBDNF) and proBDNF protein levels between WT and ALS mice in plantaris muscles from symptomatic (P115) and presymptomatic (P50) mice. We used an anti-BDNF antibody raised against a region present in both proBDNF (32 kDa) and mBDNF (14 kDa) [43]. Results showed that mBDNF is significantly increased in P115 ALS mice (3-fold) without changes in proBDNF levels (Fig. 1a). In presymptomatic mice, both forms of BDNF are unchanged. Moreover, neurotrophin-4 (NT4) is also increased ~3-fold in P115 ALS mice and, in this case, a significant increase is observed since P50 (Fig. 1a).

Then, we analyzed the BDNF/NT4 receptors, p75^{NTR} and TrkB, both expressed in WT skeletal muscle. Alternative splicing of TrkB generates full-length receptors (TrkB.FI) with strong survival effects for nervous cells and truncated receptors (TrkB.T1) without intracellular tyrosine kinase domain. We used an anti-TrkB antibody raised against a peptide sequence shared by both TrkB.FI (145–150 kDa) and TrkB.T1

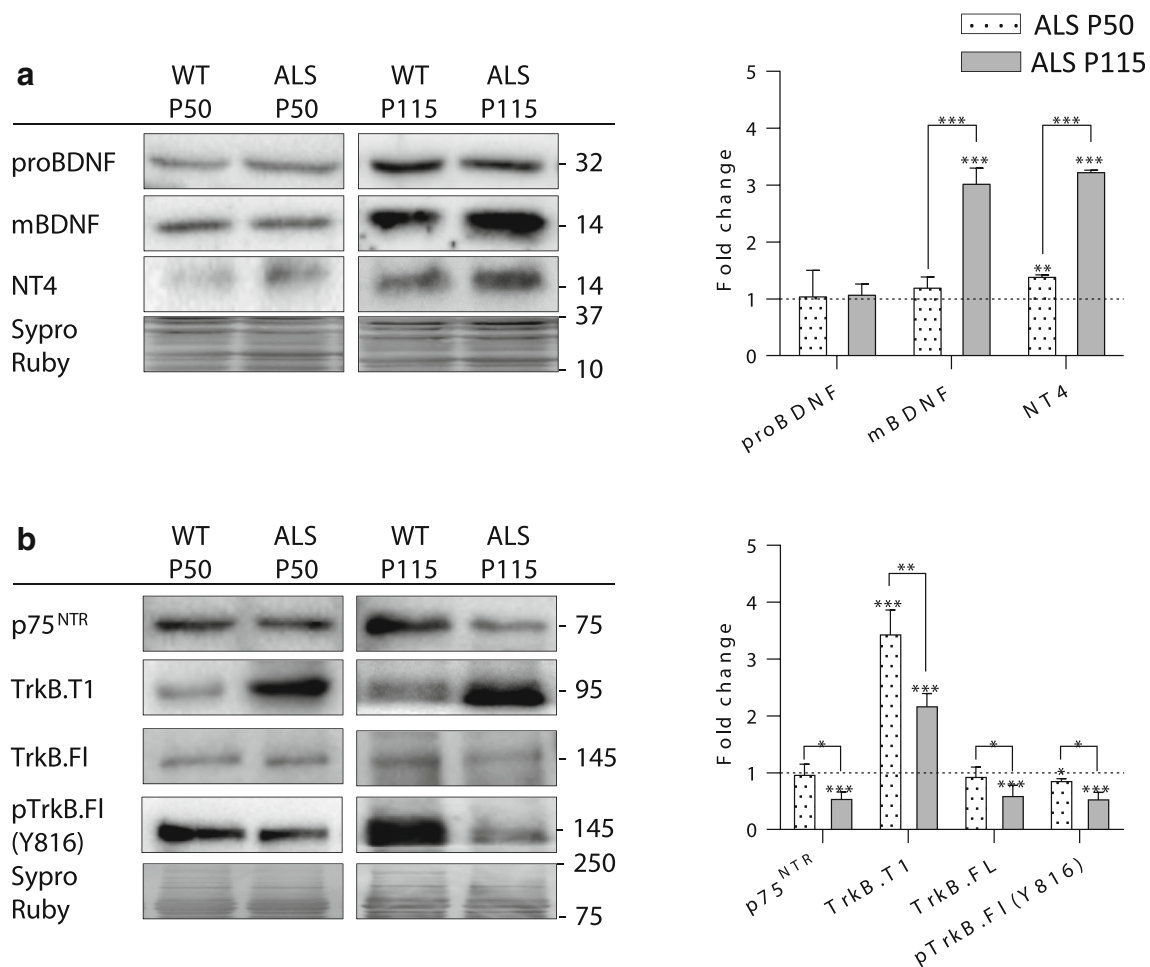


Fig. 1 BDNF, NT4 and receptors in plantaris muscles of ALS mice at P50 and P115. **a, b** Western blot bands and quantification. **a** ALS disease increases NT4 yet at P50 and mBDNF at P115 but never affects proBDNF. **b** ALS disease increases TrkB.T1 yet at P50 and decreases p75^{NTR}, TrkB.FI, and pTrkB.FI at P115. Sypro Ruby images show the region surrounding each protein of interest despite bands optical densities were normalized using the full length of the lanes. Statistical significance

was evaluated under a non-parametric Kruskal-Wallis test followed by Dunn's post hoc test. Data are mean percentage \pm SD, * $p < 0.05$, ** $p < 0.01$, *** $p < 0.001$ ($n = 5$; 3 repeats). Note: Asterisks over the columns indicate the difference between control and ALS mice while asterisks over the lines that connect columns indicate the difference between P50 and P115 mice

(95–100 kDa). Our results show that p75^{NTR} and TrkB.FI are significantly decreased in about a half in ALS P115 while TrkB.T1 is significantly increased. As a result, the FI/T1 ratio decreases about 2/3 in ALS mice at P115. Interestingly, TrkB.T1 is already increased in ALS P50, without changes in p75^{NTR} nor TrkB.FI, therefore also the FI/T1 ratio is similarly decreased at P50 (Fig. 1b; Table 2 (A. Neurotrophins and neurotrophin receptors, first line)).

Since TrkB signaling starts with the TrkB.FI phosphorylation [44], we next analyzed it and found that pTrkB.FI (Y816) is decreased in about a half in P115. However, the ratio pTrkB.FI/TrkB.FI is not affected due to the similar decrease of TrkB.FI. A moderate but significant decrease of pTrkB.FI is yet observed at P50 (Fig. 1b; Table 2 (A. Neurotrophins and neurotrophin receptors, first line)). Taken together, these results confirm that the neurotrophic pathway is altered in ALS plantaris muscles, with an increase in mBDNF and

NT4 expression and a decrease in TrkB-FI activation, probably since the presymptomatic stage, due to the precocious increase of TrkB.T1. The alteration of neurotrophic receptors and neurotrophins could decrease their intracellular signaling.

Serine-Threonine Kinases

TrkB.FI (Y816) phosphorylation triggers the gamma phospholipase C (PLC γ) signaling pathway, which sequentially activates PKCs [45]. Because of that, we next analyzed the protein levels of representative serine-threonine kinases: the ubiquitous cPKC α and the presynaptic cPKC β I and nPKC ϵ and also the PKA subunits. All of them have been functionally related to the BDNF/TrkB receptor complex in the presynaptic component of the NMJ [28, 30, 40, 41, 46, 47].

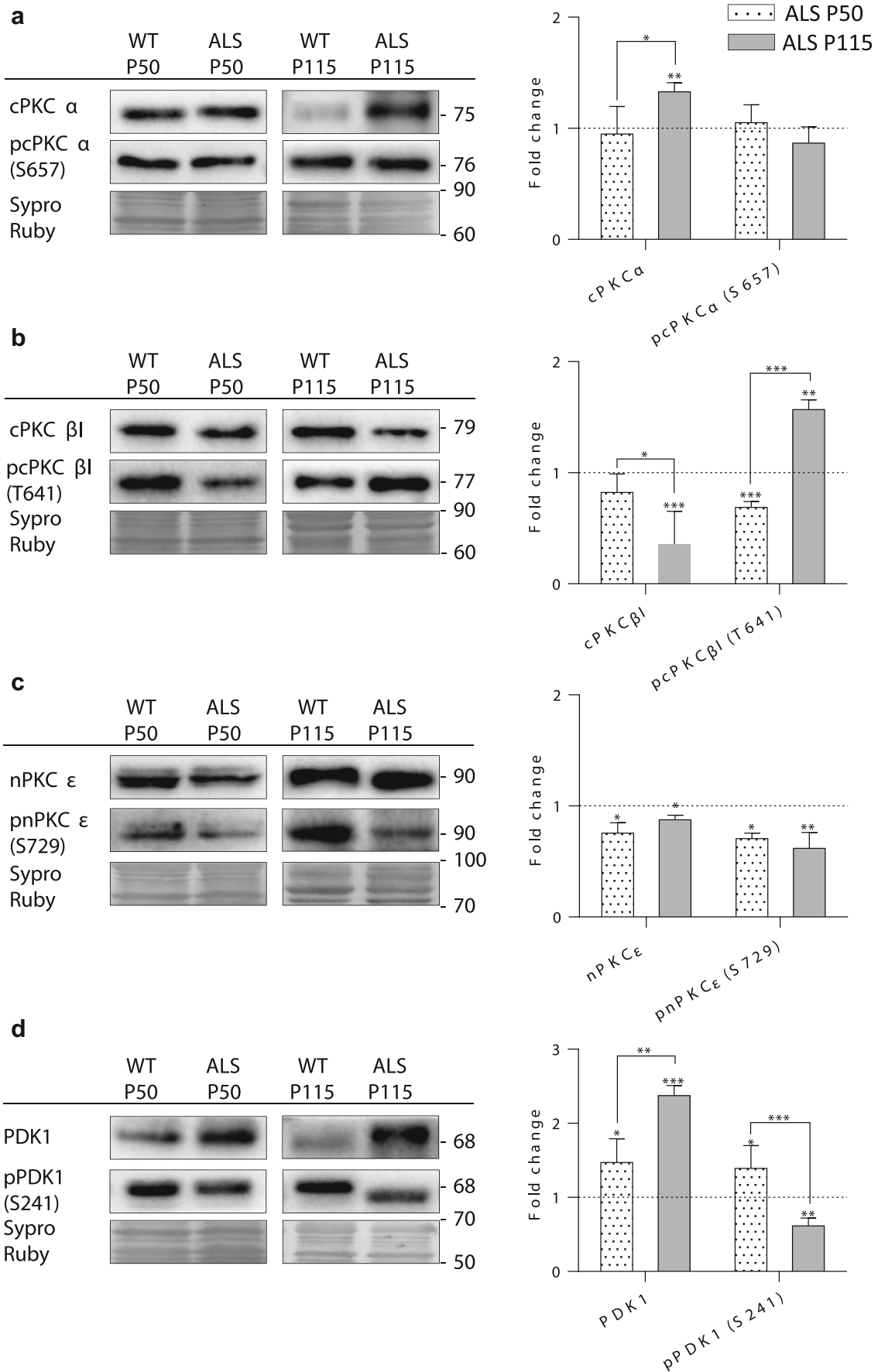


Fig. 2 cPKC α , cPKC β I, nPKC ϵ and PDK1 in plantaris muscles of ALS mice at P50 and P115. **a–d** Western blot bands and quantification. **a** cPKC α increases at P115. **b** cPKC β I decreases at P115 while pcPKC β I decreases at P50 and increases at P115. **c** nPKC ϵ and nPKC ϵ decrease at P50 and P115. **d** PDK1 increases yet at P50 but pPDK1 decreases at P115. Sypro Ruby images show the region surrounding each protein of interest despite bands optical densities were normalized using the full length of the lanes. Statistical significance was evaluated under a non-parametric Kruskal-Wallis test followed by Dunn's post hoc test. Data are mean percentage \pm SD, * $p < 0.05$, ** $p < 0.01$, *** $p < 0.001$ ($n = 5$; 3 repeats). Note: Asterisks over the columns indicate the difference between control and ALS mice while asterisks over the lines that connect columns indicate the difference between P50 and P115 mice

PKC

Total cPKC α protein levels increase without affecting the phosphorylated form at P115 (Fig. 2a). Moreover, cPKC β I decreases while pcPKC β I increases in P115 ALS muscles. In contrast, at P50 only pcPKC β I significantly decreases (Fig. 2b). Finally, nPKC ϵ and pnPKC ϵ decrease both at P115 and P50 (Fig. 2c). This indicates that ALS differently

affects the three PKC isoforms in plantaris muscles. When considering the ratio “phosphorylated/total protein” of these kinases, we observed that at P50, pcPKC α /cPKC α , pcPKC β I/cPKC β I, and pnPKC ϵ /nPKC ϵ do not change, suggesting that at the presymptomatic stage the potential efficacy of the kinase activity is barely affected. On the other hand, at P115, pcPKC β I/cPKC β I increases more than 4-fold while pnPKC ϵ /nPKC ϵ and pcPKC α /cPKC α show a moderate decrease (Table 2 (B. Downstream protein kinase C (PKC) signaling, first line)).

PKC maturation includes three phosphorylation steps and the first one is mediated by phosphoinositide-dependent kinase-1 (PDK1). Previous results showed that PDK1 is exclusively located in the nerve terminal of the NMJ and that synaptic activity enhances pPDK1 (S241) in the membrane, where it realizes its function [41]. Here, we found that PDK1 increases about 2.5-fold and pPDK1 decreases about 1/3 at P115 while an increase of 0.5-fold is observed in both molecules at P50 (Fig. 2d). Thus, this result points to an imbalance of the pPDK1 and its substrate pcPKC β I that

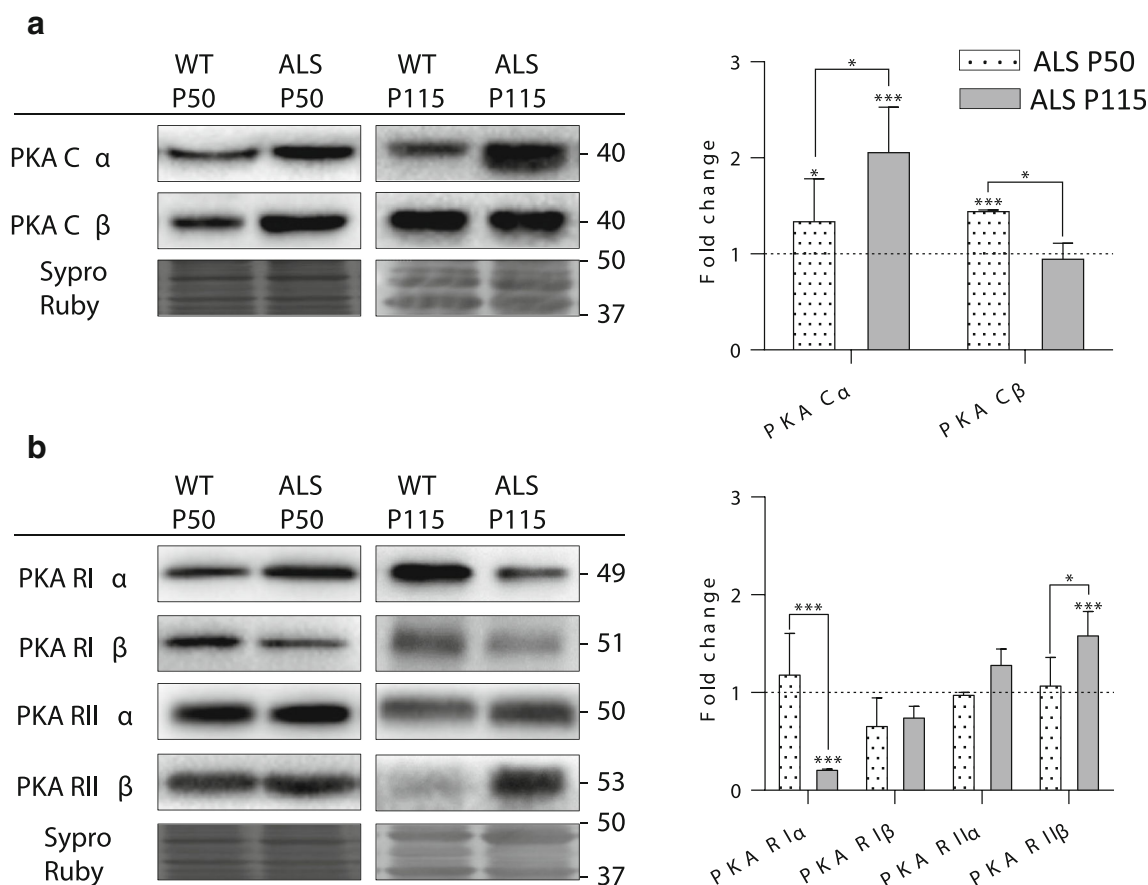


Fig. 3 Catalytic and regulatory PKA subunits in plantaris muscles of ALS mice at P50 and P115. **a, b** Western blot bands and quantification. **a** Catalytic C α increases yet at P50 and C β is increased only at P50. **b** Regulatory RI α decreases and RII β increases at P115 without any change in the other subunits. Sypro Ruby images show the region surrounding each protein of interest despite bands optical densities were normalized

using the full length of the lanes. Statistical significance was evaluated under a non-parametric Kruskal-Wallis test followed by Dunn's post hoc test. Data are mean percentage \pm SD, * $p < 0.05$, ** $p < 0.01$, *** $p < 0.001$ ($n = 5$; 3 repeats). Note: Asterisks over the columns indicate the difference between control and ALS mice while asterisks over the lines that connect columns indicate the difference between P50 and P115 mice

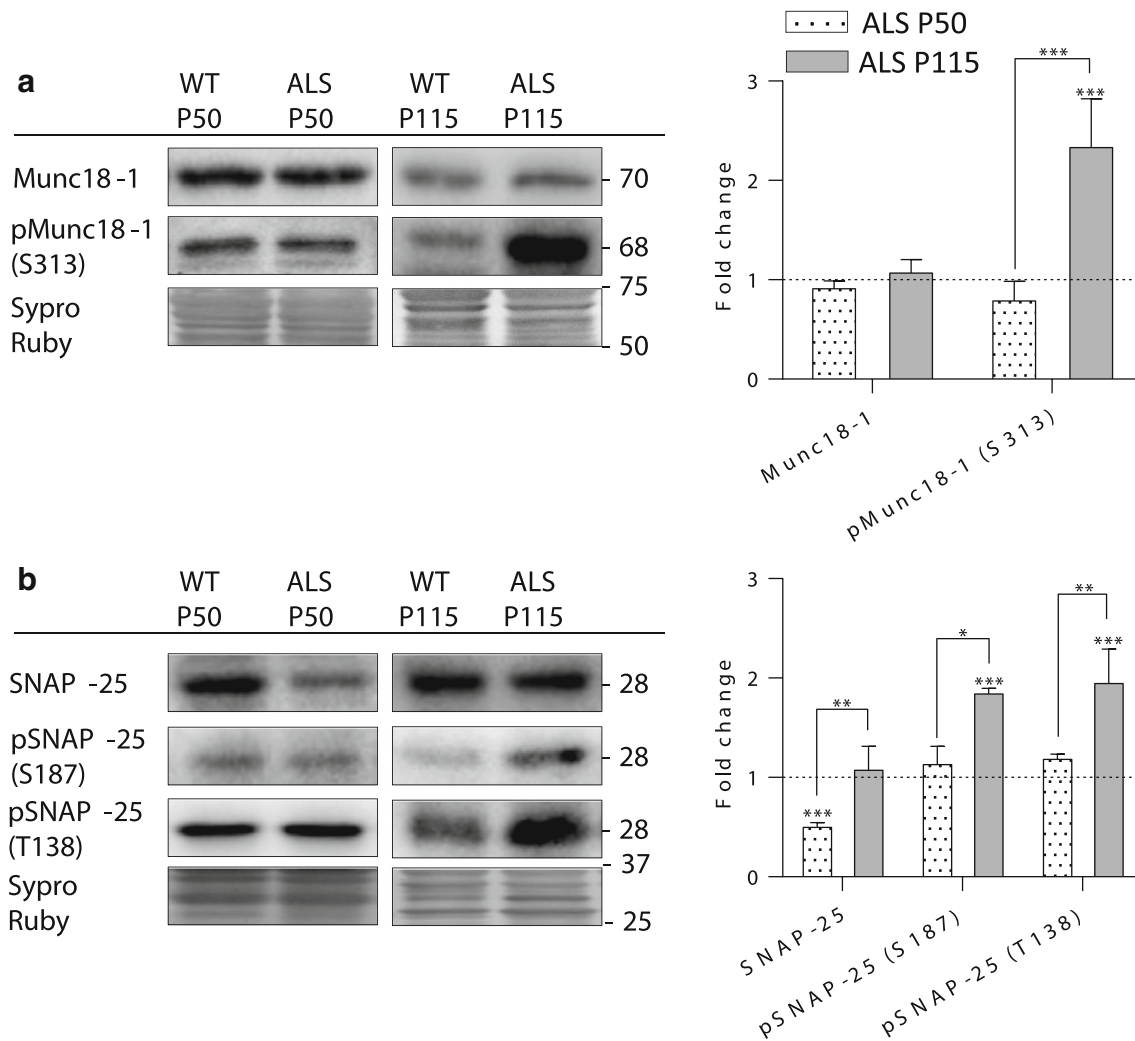


Fig. 4 The SNARE/SM Munc18-1 and SNAP-25 in plantaris muscles of ALS mice at P50 and P115. **a, b** Western blot bands and quantification. **a** pMunc18-1 increases at P115. **b** SNAP-25 is decreased only at P50; pSNAP-25 (S187) and (T138) increase at P115. Sypro Ruby images show the region surrounding each protein of interest despite bands optical densities were normalized using the full length of the lanes. Statistical

significance was evaluated under a non-parametric Kruskal-Wallis test followed by Dunn's post hoc test. Data are mean percentage \pm SD, * $p < 0.05$, ** $p < 0.01$, *** $p < 0.001$ ($n = 5$; 3 repeats). Note: Asterisks over the columns indicate the difference between control and ALS mice while asterisks over the lines that connect columns indicate the difference between P50 and P115 mice

highlights the affectation of cPKC β I in symptomatic ALS and suggest PDK1-independent modulation of the cPKC β I phosphorylation.

PKA

Regarding PKA subunits, the regulatory ones do not change at P50 whereas the catalytic subunits C α and C β increase moderately and, at P115, only C α significantly increases (2-fold, Fig. 3a). Moreover, RII α significantly decreases (about 2/3) accompanied by a significant increase of the RII β subunit (of 2-fold) (Fig. 3b).

These results suggest a change in the pattern of activation of the PKA pathway, which could modulate downstream phosphorylation targets implicated in synaptic function.

SNARE/SM Proteins

We next analyzed different representative targets of PKC and PKA closely related with the exocytotic machinery: the regulatory SM family protein, Munc18-1 and the SNARE protein, SNAP-25.

Table 2 Protein levels in different muscles in relation with WT plantaris (P115)

	Neurotrophins and neurotrophin receptors							Ratios				
	proBDNF	mBDNF	NT4	p75 ^{NTR}	TrkB.T1	TrkB.FL	pTrkB.FI (Y816)	mBDNF/proBDNF	mBDNF/NT4	pTrkB.FI (Y816)/TrkB.FI	TrkB.FI/TrkB.T1	
ALS Plantaris	1.06 ± 0.20 ns	3.01 ± 0.29 ***	3.22 ± 0.04 ***	0.53 ± 0.13 ***	2.16 ± 0.24 ***	0.58 ± 0.19 ***	0.52 ± 0.14 ***	2.84 ± 0.59 ***	0.94 ± 0.09 ns	0.89 ± 0.37 ns	0.27 ± 0.09 **	
WT Soleus	1.05 ± 0.31 ns ns ns	0.57 ± 0.27 * # + + +	1.89 ± 0.03 *** ns + + +	1.11 ± 0.03 ns ns + + +	0.92 ± 0.06 ns ns + + +	0.63 ± 0.04 ** # # ns	0.19 ± 0.01 *** # # # ns	0.55 ± 0.28 * # + +	0.30 ± 0.15 *** ns + + +	0.30 ± 0.03 *** # # + +	0.68 ± 0.06 ** ns + +	
WT Tibialis	0.97 ± 0.18 ns	1.08 ± 0.01 ns	2.37 ± 0.23 ***	0.99 ± 0.27 ns	1.11 ± 0.10 ns	1.06 ± 0.20 ns	0.99 ± 0.31 ns	1.11 ± 0.20 ns	0.46 ± 0.04 **	0.93 ± 0.34 ns	0.95 ± 0.20 ns	

	Downstream Protein Kinase C (PKC) signaling								Ratios				
	PDK	pPDK (S241)	cPKCα	pcPKCα (S657)	cPKCβ	pcPKCβ (T641)	nPKCε	pnPKCε (S729)	pPDK (S241)/PDK	pcPKCα (S657)/cPKCα	pcPKCβ (T641)/cPKCβ	pnPKCε (S729)/nPKCε	
ALS Plantaris	2.38 ± 0.13 ***	0.62 ± 0.11 **	1.33 ± 0.08 **	0.87 ± 0.15 ns	0.36 ± 0.29 ***	1.57 ± 0.09 **	0.88 ± 0.14 *	0.62 ± 0.14 **	0.26 ± 0.05 ***	0.65 ± 0.12 *	4.37 ± 3.60 **	0.71 ± 0.17 **	
WT Soleus	1.35 ± 0.09 ns ns + + +	0.99 ± 0.26 ns ns ns	1.19 ± 0.01 ns ns ns	0.61 ± 0.03 ** ns ns	0.15 ± 0.11 *** # # ns	0.51 ± 0.22 *** ns + + +	1.65 ± 0.32 ns ns +	0.77 ± 0.06 ns ns ns	0.74 ± 0.20 ns ns +	0.51 ± 0.03 *** ns ns	3.43 ± 2.96 * # ns	0.46 ± 0.10 ** ns ns	
WT Tibialis	1.19 ± 0.02 ns	0.91 ± 0.21 ns	1.08 ± 0.38 ns	0.83 ± 0.18 ns	0.60 ± 0.31 **	0.77 ± 0.03 ns	1.48 ± 0.06 ***	1.01 ± 0.28 ns	0.77 ± 0.18 ns	0.77 ± 0.32 ns	1.28 ± 0.65 ns	0.69 ± 0.19 *	

	Protein Kinase A (PKA) Subunits					
	PKA Cα	PKA Cβ	PKA R1α	PKA R1β	PKA R1α	PKA R1β
ALS Plantaris	2.06 ± 0.47 ***	0.94 ± 0.17 ns	0.20 ± 0.01 ***	0.74 ± 0.12 ns	1.28 ± 0.17 ns	1.58 ± 0.25 ***
WT Soleus	2.04 ± 0.07 *** # # # ns	1.13 ± 0.43 ns # ns	2.40 ± 0.56 *** # # # + + +	1.15 ± 0.01 ns ns +	0.79 ± 0.09 ns ns ns	1.98 ± 0.07 ** ns ns
WT Tibialis	0.85 ± 0.00 ns	0.68 ± 0.14 *	1.13 ± 0.58 ns	1.64 ± 0.28 *	0.76 ± 0.19 ns	1.44 ± 0.13 *

	SNARE/SM proteins					Ratios		
	Munc18-1	pMunc18-1 (S313)	SNAP-25	pSNAP-25 (S187)	pSNAP-25 (T138)	pMunc18-1 (S313)/Munc18-1	pSNAP-25 (S187)/SNAP-25	pSNAP-25 (T138)/SNAP-25
ALS Plantaris	1.07 ± 0.13 ns	2.33 ± 0.49 ***	1.07 ± 0.24 ns	1.84 ± 0.06 ***	1.95 ± 0.35 ***	2.18 ± 0.53 *	1.73 ± 0.39 *	1.82 ± 0.52 *
WT Soleus	0.75 ± 0.12 ns ns ns	0.54 ± 0.11 *** # # # + + +	0.75 ± 0.17 ns ns ns	2.31 ± 0.06 *** # # # ns	0.35 ± 0.21 *** # # # + + +	0.72 ± 0.18 * ns + +	3.08 ± 0.69 *** # # # + + +	0.46 ± 0.29 *** # # # + + +
WT Tibialis	1.02 ± 0.13 ns	1.07 ± 0.14 ns	0.95 ± 0.10 ns	1.13 ± 0.01 ns	1.68 ± 0.32 ***	1.05 ± 0.19 ns	1.19 ± 0.13 ns	1.77 ± 0.39 *

a. Differential pattern of the TrkB signaling molecules. b. PDK1 and PKC isoforms. c. PKA catalytic and regulatory subunits. d. SNARE/SM proteins Munc18-1 and SNAP-25. The numerical data show the mean ± SD of the considered molecules in ALS plantaris, WT soleus and WT tibialis in relation with WT plantaris muscle, whose value has been normalized to 1. In blue, the molecules that in the ALS plantaris muscles become similar to the values in the WT soleus. In yellow, the molecules that in the ALS plantaris muscles are different from WT soleus. The molecules that do not change are in white. Statistical significance was evaluated with the non-parametric Kruskal-Wallis test followed by Dunn's post hoc test and with the Friedman test followed by a Bonferroni correction.

Significant differences between the muscles and WT plantaris; # significant differences between WT soleus and WT tibialis; + significant differences between ALS plantaris and WT soleus ($p < 0.05$; ** $p < 0.01$; *** $p < 0.001$; not significant (ns))

Munc18-1

Munc18-1, is a neuron-specific member of the Sec1/Munc18 protein family (SM family) that binds to syntaxin-1 and regulates the formation of the SNARE/SM complex [48–54]. It has two targets for PKCs (Serine 306 and 313) that change its conformation to enhance exocytosis [55–59].

Results show a significant increase of pMunc18-1 (S313) (of more than two-fold) in P115 ALS plantaris, whereas total Munc18-1 does not change. Therefore, pMunc18-1/Munc18-1 ratio increases. These results indicate that in symptomatic ALS mice, Munc18-1 phosphorylation is enhanced, resulting in the upregulation of the synaptic exocytotic machinery. This points out the

complex dysregulation of this molecule at the end stage of the disease, as they do not change at P50 (Fig. 4a).

SNAP-25

SNAP-25 is one of the three SNARE proteins of the core fusion machine implicated in vesicle exocytosis. PKA-mediated phosphorylation of SNAP-25 at T138 controls the size of the releasable vesicle pools and PKC-mediated phosphorylation at S187 regulates pool refilling after they have been emptied [60, 61].

SNAP-25 levels decrease at P50, but they are recovered at P115. pSNAP-25S187 and T138 are unaffected at P50, but they increase (almost 2-fold in both cases) at P115 (Fig. 4b). As a consequence, when considering the ratio phosphorylated/total protein, the data show an increase both at P50 (the ratios pSNAP-25S187/SNAP-25 and pSNAP-25T138/SNAP-25 are increased: 2.28 ± 0.43 and 2.38 ± 0.26 respectively, $p < 0.05$ in both cases) and P115 (due to pSNAP-25S187 and T138 increase) (Table 2 (D. SNARE/SM proteins, first line)). This indicates a good phosphorylating efficacy of both PKC and PKA on SNAP-25 along the disease progression which suggests that the changes in the kinases modulate SNAP-25 phosphorylation to influence neurotransmission in ALS plantaris muscles at the end stage of the disease.

Differential Expression of the BDNF/TrkB/PKC Signaling in Slow and Fast-Twitching Muscles

Considering the preferential degeneration of the fast motor units in ALS progression and the fast-to-slow transition of the muscle phenotype, we wondered whether the above-exposed molecular changes at the end stage of the disease could be related to this transition, or, by the contrary, be specific of ALS. To assess this, we compared slow-twitching muscles with fast-twitching ones in WT animals. This allowed us to relate the values of slow WT muscles with the fast ALS ones.

Table 2 (A. Neurotrophins and neurotrophin receptors) sums up the differential pattern of the neurotrophic pathway. The WT slow soleus muscle has lower levels of mBDNF, TrkB.F1, and pTrkB.F1 than the WT fast plantaris muscle. Also, in comparison, soleus has less cPKC β I and pPKC β I and more nPKC ϵ (Table 2 (B. Downstream protein kinase C (PKC) signaling)). PKA catalytic and regulatory subunits C α , RI α , and RII β levels are higher in WT soleus (Table 2 (C. Protein kinase A (PKA) subunits)). Finally, there is less Munc18-1, pMunc18-1, SNAP-25, and pSNAP-25 (T138) but more pSNAP-25 (S187) in the soleus muscle (Table 2 (D. SNARE/SM proteins)). In addition to the WT plantaris, we included WT tibialis as a control in the comparisons. Interestingly, the value of some molecules in this muscle are

different from the plantaris (see Table 2 (A. Neurotrophins and neurotrophin receptors, B. Downstream protein kinase C (PKC) signaling, C. Protein kinase A (PKA) subunits, and D. SNARE/SM proteins)) which could be attributed to specific muscle fiber composition and should be further investigated.

Thus, there are evident differences in the molecular pattern of the studied signaling pathway between WT fast and slow muscles. In Table 2, the protein values in the ALS plantaris that become similar to the values in the WT soleus muscles are indicated in blue. This similarity may be related to the fast-to-slow transition caused by ALS and may represent the part of the pathway that works to prevent the complete loss of NMJ. On the contrary, the protein values that are different in ALS plantaris and WT soleus muscles or that go in another direction when compared with the plantaris WT are highlighted in yellow. This dissimilarity may be related not with the fast-to-slow transition but with another ALS mechanism closely related with the cause of the disease. Fig. 6b (2) shows a diagrammatic representation of these results.

Motoneuron Loss in P115 ALS Mice Spinal Cord

It is described that ALS involves loss of MNs, preferentially the larger ones innervating faster muscle fibers that are the ones that change their phenotype [32, 33]. In the context of the present study, we confirmed this selective loss of larger-fast MN. We analyzed the changes in the percentage of fast (larger) and slow (smaller) MN in the spinal cord of the symptomatic ALS mice (115 days old) compared with WT animals (Fig. 5). When analyzing soma's area, we observed an increase of the 300–900 μm^2 MN (mainly slow) from 25 to 40% whereas the percentage of higher of 900 μm^2 MN (mainly fast) diminishes from 25 to 15%. Thus, in the studied spinal cord of ALS mice, the proportion of small (and therefore mainly slow) MN increases.

Discussion

Neurotrophic dysfunction at the NMJ influences its stability and may contribute to motor impairment in ALS muscles. The present results show that ALS disease strongly alters, in the plantaris muscle, at the presymptomatic stage but mainly in symptomatic animals, protein and phosphorylation levels of many molecules of the putative BDNF-NT4/TrkB-p75^{NTR}/PKC-PKA/SNARE-SM pathway, which is essential to modulate NMJ maintenance and promote neurotransmission. These complex changes are represented in the intuitive graphic of Fig. 6 and, despite that the relations between molecular changes

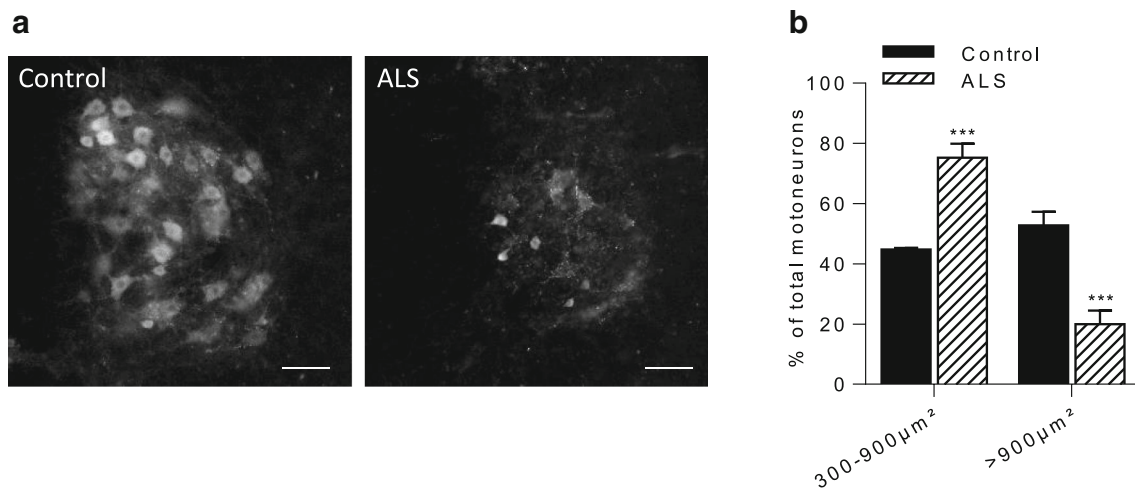


Fig. 5 Motoneurons in the spinal cord of WT and ALS mice at P115. **a** MN stained with ChAT in a WT mice (right) and in a SOD1-G93A mice (left). The bar indicates 50 μm . **b** The proportion of large (fast) and small (slow) MN in the spinal cord of the symptomatic (115 days old) SOD1-G93A mice compared with the WT ones at the same days old. The

percentage of 300–900 μm^2 MN (slow) increase in the ALS spinal cord whereas the percentage of >900 μm^2 MN (mainly fast) diminishes. Statistical significance was evaluated under a non-parametric Mann-Whitney *U* test followed by Holm-Sidak post hoc test. Data are mean percentages \pm SD, *** $p < 0.001$ ($n = 5$; 6 sections per n)

may not be evident, we discuss their meaning that (I) may be specific of ALS pathogenesis or (II) can be explained by the fast-to-slow fiber transition.

The TrkB Signaling

The functional isoform of TrkB receptor is TrkB.FI. However, the truncated TrkB.T1 is the predominant form in mammalian skeletal muscle [14]. It affects cellular viability when it is over-expressed in artificial or pathological situations [62] and negatively regulates TrkB.FI, consequently affecting its signaling.

ALS patients have increased BDNF and NT4 in skeletal muscle and spinal cord and decreased pTrkB.FI [23, 63]. Our results confirm these neurotrophins increase (even in pre-symptomatic mice, in the case of NT4), the decrease of pTrkB.FI (since P50 and due to the loss of total TrkB.FI protein levels in symptomatic mice) and, additionally, the great TrkB.T1 increase in the plantaris skeletal muscle in both stages. The early deregulation of TrkB alternative splicing—yet in presymptomatic animals—may lead to an impaired neuromuscular function which could underlie motoneuron loss. This suggestion is supported by experiments in which TrkB.T1 deletion in mutant SOD1 mice delays the onset of the disease, slows down the motoneuron loss and improves mobility tests results at the end stage of the disease compared with normal mutant SOD1 mice [22]. In addition, the deletion of TrkB.T1 increases neuromuscular function and nerve-evoked muscle contraction [62]. Altogether, it can be suggested that the over-presence of TrkB.T1 limits BDNF and NT4 effect by hijacking it and prevents its action through TrkB.FI, with a direct impact on the signal transduction, despite being overproduced. Because of that, it seems that the

increase of BDNF and NT4 in ALS is an insufficient compensatory mechanism to promote neuronal survival of injured motoneurons because of the lack of TrkB.FI available, as it has already been proposed in other studies [22]. Also, p75^{NTR} is strongly related with cell death and neurodegeneration in the adult nervous system. In fact, different results have found that under high doses of neurotrophins, p75^{NTR} acquires a proapoptotic role which goes through the activation of caspase 3 [20, 64]. Therefore, it seems to be also directly related with ALS process despite of its total levels being decreased.

Enhancement of BDNF signaling may have a great potential in therapy for neurological disorders like ALS, due to its strong pro-survival effects through TrkB and p75^{NTR} in developing and injured MN [25, 65, 66]. However, intrathecally administered BDNF did not show significant effects on motor function and survival in ALS patients [67] or autonomic nervous system function [68]. Here, we reveal that ALS not only shows a timely dysregulation of the ligands but also of the receptors which suggest an early alteration of the alternative splicing of the TrkB.

In summary, the neurotrophic signaling that under normal conditions guarantees the stability and functionality of the NMJ through synaptic activity [14] is highly and precociously affected in ALS. As a result, the long-term compensatory increase of neurotrophins is not sufficient due to the TrkB.T1 dominance since the presymptomatic stage of the disease.

PKC and PKA in ALS Muscle

TrkB.FI stimulates the PLC γ , which activates PKC [14, 44, 45, 69]. Therefore, when TrkB.FI is downregulated (as it happens in ALS), the PKC activation may be decreased or lost. Here, we analyzed three PKC isoforms (α , β I, and ϵ ; the last

two are exclusively presynaptic) which are upregulated by synaptic activity and muscle contraction through BDNF/TrkB signaling [14, 28, 30] to control the neuromuscular function [14, 29].

Surprisingly, in ALS symptomatic muscles, the phosphorylation of these PKCs do not change (cPKC α), increase (cPKC β I), or even decrease (nPKC ϵ). Thus, a relevant modification in the normal balance of the β I and ϵ isoform activity can be intuited. Interestingly, the pcPKC β I increase is accompanied with a reduction in total cPKC β I protein and the pnPKC ϵ decrease occurs in parallel with a reduction in nPKC ϵ , thus, increasing the evidences of the dysregulation between PKC isoforms. Moreover, cPKC α increases and, therefore, the ratio pcPKC α /cPKC α is reduced. Altogether, whereas the ratio phosphorylated/non-phosphorylated form of α and ϵ isoforms is reduced and not modified respectively in the ALS symptomatic muscle, it strongly increases for β I isoform. The normally constitutive upstream kinase for PKCs (PDK1) is highly altered in ALS muscles and may influence the changes in PKC isoforms phosphorylation. All these results suggest an increased activity and consumption of cPKC β I whereas nPKC ϵ activity decreases. Both kinases regulate the neuromuscular transmission [14, 29] and, therefore, their imbalance could directly affect it. In accordance, our results in the ALS plantaris muscle show that the imbalance of the levels of PKC isoforms coincide with a significative increase in the protein levels of PKC-mediated phosphorylations of Munc18-1 and SNAP-25 (in the Ser-313 and Ser-187, respectively; see later), indicating a dysregulation of the exocytotic synaptic machinery. The modification of the normal balance of PKC isoforms and PDK1 have already been observed in presymptomatic ALS muscles. Changes at P115 for nPKC ϵ are already found at P50, while pPDK1 and pPKC β I modifications are opposed to the ones that occurred at P50, suggesting their profound and complex alteration in the progression of the disease.

The changes in the balance of the presynaptic PKC isoforms may be related with the imbalance of the TrkB isoforms. However, it could be suggested that other presynaptic metabotropic receptors related with PLC γ or PLC β (such as adenosine receptor A $_1$ and muscarinic receptor M $_1$) may contribute to the selective modulation of different PKC isoforms in the muscle, and this must be investigated because their activity is related with TrkB and PKC [12, 70, 71].

Neurons affected by ALS have high Ca $^{2+}$ concentrations, which has been related with apoptosis induction due to ion imbalance [72, 73] and sustained calcium-dependent PKC activation [74]. Also, immunohistochemical analyses have reported a decrease of PKCs in spinal cord motoneurons affected by ALS, which has been associated with a selective degeneration of the largest motoneurons [75]. These changes are in accordance with the

decrease of cPKC β I and nPKC ϵ that we found in the symptomatic skeletal muscle.

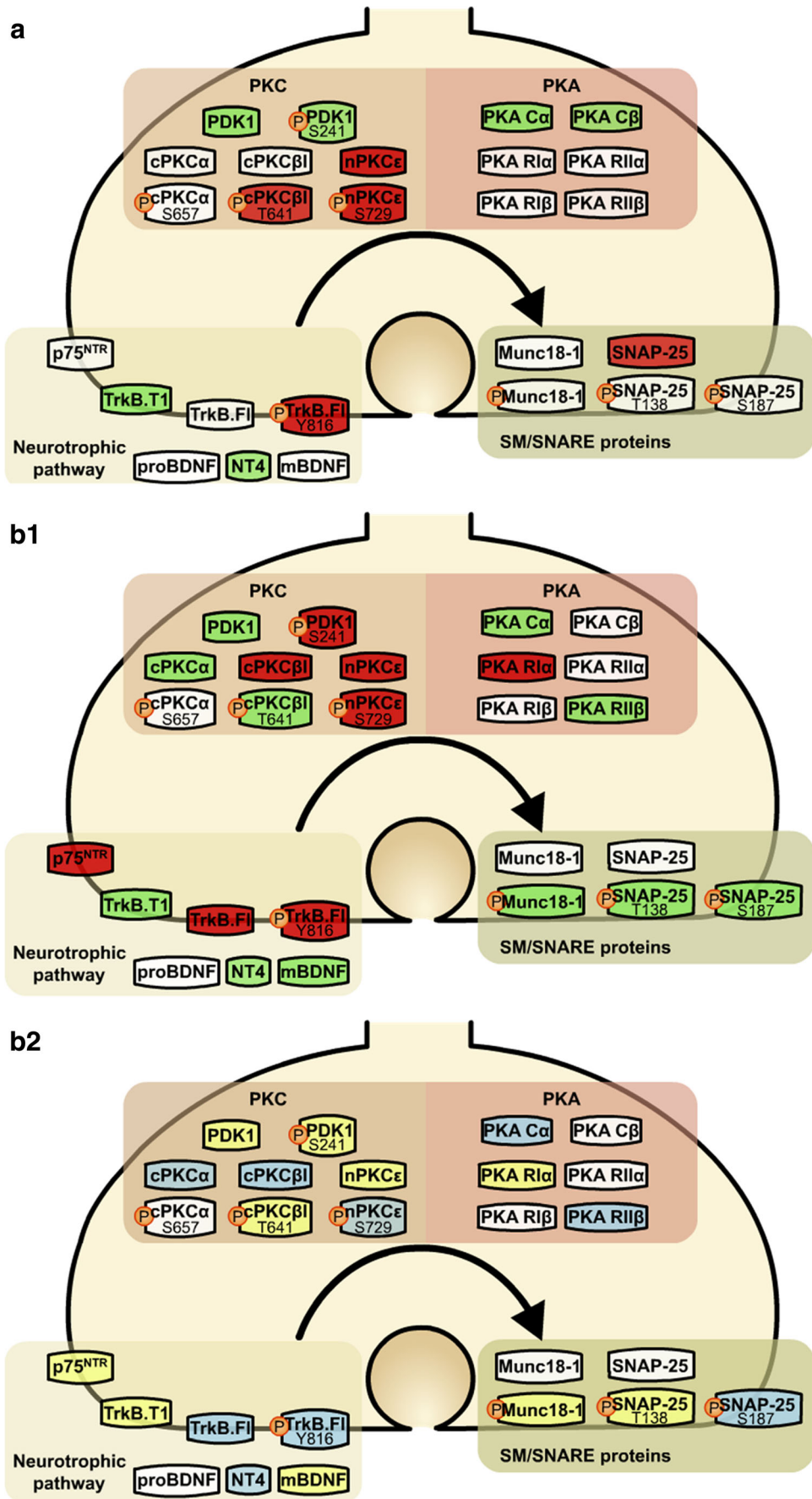
On the other hand, the increase of the catalytic PKA isoforms (both at P50 and P115) together with maintenance of the total count of RI and RII regulatory isoforms could be the reason why pSNAP-25T138 is increased in symptomatic ALS mice. This could be due to the impossibility of RI α to modulate PKA activity in this situation, as it is known that it works as a buffer to modulate it in normal conditions [76, 77]. These results coincide with previous studies done in the central nervous system, where total PKA was increased not only in mice and rats but also in human patients [78, 79] therefore contributing to the changes in neurotransmission that occur in ALS muscles.

Exocytotic Synaptic Proteins in ALS Muscle

cPKC β I, nPKC ϵ , and PKA subunits regulate the neuromuscular synapse [14, 40]. Therefore, their changes may influence neurotransmission in ALS. In the presymptomatic phase, endplate potentials (EPP) amplitude and quantal content are increased, suggesting an abnormal upregulation in Ca $^{2+}$ levels in the nerve terminals [80]. In spite of the important changes in neurotrophin and kinases signaling described, only SNAP-25 expression is reduced to the half at P50. However, the ratios pSNAP-25S187/SNAP-25 and pSNAP-25T138/SNAP-25 are high, indicating a good phosphorylating efficacy of both PKC and PKA on SNAP-25. These data, in concordance with unchanged levels of pMunc18-1 in this presymptomatic stage, indicate a good operation of vesicle release to support the high quantal content in presymptomatic stage.

At the same time that the disease progresses and the large MN die, the EPPs amplitude and quantal release is reduced [81, 82]. This phenomenon could be in part due to the fast-to-slow transition because the small and slow MN generate EPP with smaller quantal content than big and fast MN [83]. In fact, the ALS plantaris muscle at P115 show a significative increase in the protein levels of pSNAP-

Fig. 6 Overview of the molecular changes in the ALS muscles at P50 and P115. **a b** (1) In red, the molecules that are decreased; in green, the ones that are increased and in white the ones that are not changed. In **(a)**, the molecular changes at P50 are represented. Most molecules are unaffected despite some changes begin to appear. In **(b)**, the molecular changes at P115 are represented. There are profound alterations in the BDNF/TrkB receptor complex, in their coupled serine-threonine kinases and in the main related synaptic vesicle fusion protein targets. **b** (2) In blue, the molecules that would have followed a fast-to-slow transition (and, therefore, resemble WT soleus) and in yellow the ones that have not (different to WT soleus), at P115. This dissimilarity may indicate an adaptation of the motor units beyond the fast-to-slow transition in the ALS context. Alternatively, they may represent a molecular alteration related to the primary cause of the disease. The molecules that do not change are indicated in white. In **(a)** and **(b** (1 and 2)), the black arrow indicates the normal downstream signaling, from the receptors to the exocytotic machinery going through the different serine-threonine kinases



25S187 in a similar way to the slow WT soleus. However, pSNAP-25T138 and pMunc18-1S313 are also really increased contrarily to soleus. Therefore, the ratio phosphorylated/total protein of the three molecules is very high in ALS P115, maybe because the remaining motoneurons generate bigger amounts of pMunc18-1 and pSNAP-25 to maintain neurotransmission, but they accumulate and do not do their function.

Fast-to-Slow Transition in the ALS Fast-Twitching Muscles

The molecular changes observed in end-phase ALS mice may be related either with the cause of the disease, the consequence or a combination of both. Motoneuron loss occurs in the ventral horns of the symptomatic ALS animals mainly affecting medium and large somas and muscle phenotype changes in parallel with it. In the fast-twitch muscles (like the plantaris), there is a significant fast-to-slow transition from type II fibers to type I fibers and, within the type II fiber population, from type IIb/IIx to IIa fibers [32, 33]. In accordance, a fat mass reduction and weight loss, together with altered energy metabolism has been observed both in animal models and human patients [84]. These changes occur before the first motor symptoms in mice [85] and have been related with a switch of the source of energy of the cells from carbohydrates to lipids [86]. Some of the changes we observed at P115 resemble the molecular pattern of slow muscles like the wild soleus (Table 2 and Fig. 6b (2), in blue), which could be a side effect of the fast-to-slow transition. Some molecular differences between WT soleus (slow) and WT plantaris (fast) observed in this study can be related with the differences in quantal content of transmitter release, that is approximately a 30–40% higher in fast-twitch muscles than in slow-twitch muscles contributing to the higher safety factor in the fast NMJ [83, 87]. In the slow WT soleus, low levels of pSNAP-25 (T138) may be related with a small releasable pool of vesicles whereas the high level of pSNAP-25 (S187) may be related with constant refilling after the pools have been emptied to sustain tonic stimulation of the slow muscle during extended day use [60]. As stated, a high level of pSNAP-25 (S187) similar to the soleus is observed in the P115 ALS plantaris.

On the other hand, there are several molecules in the ALS plantaris muscles with a very different value not only from the WT plantaris muscles but also from the WT soleus muscles (Table 2; Fig. 6b (2), in yellow). These molecular changes may represent an adaptative effort to go beyond the fast-to-slow transition trying to ameliorate the increasing impairment of the neuromuscular function. Because the described molecular pattern in the P115 ALS plantaris muscles belongs to the more resistant motor units, which have survived the course of the disease process, it can be speculated that the survival capacity may be linked with these independent changes.

Decreased levels of p75^{NTR} could indicate less proapoptotic activity, whereas elevated pcPKC β I, low PKA RI α (inhibitory), and elevated values of pMunc18-1 and pSNAP-25 (T138), may represent adaptations to improve function and favor transmitter release and neurotransmission.

Finally, some of the molecular changes observed during the disease progression at the NMJ could be directly related with the etiology of ALS. Between many possible causes, a genetic (or epigenetic, in sporadic ALS) change in the free-radical defense enzyme SOD1 could be detrimental for p75^{NTR} and TrkB expression and turnover in MNs or NMJs (as shown here) and impair neuromuscular activity.

Conclusions

In ALS disease, NMJ degeneration appears before MN death, suggesting that the loss of a correct nerve-muscle contact could be a primary cause of ALS. One of the most important mechanisms involved in NMJ stability is the BDNF-NT4/TrkB neurotrophic signaling, which suffers several changes in the pre- (P50) and symptomatic (P115) SOD1-G93A mice model's plantaris muscle. The main changes are the misbalance between (i) neurotrophins (BDNF and NT4), the different TrkB receptor isoforms and the p75^{NTR} receptor, (ii) their coupled PKC isoforms themselves (presynaptic cPKC β I and nPKC ϵ) and their upstream priming kinase PDK1, (iii) the PKA catalytic and regulatory subunits and iv) the targets Munc18-1 and SNAP-25 phosphorylation. The increase of NT4 and TrkB.T1 and the decrease of the PKC isoforms already occur in presymptomatic mice. The molecular pattern observed in symptomatic ALS plantaris muscles may be partially explained by the fast-to-slow fiber transition, which affects the motor units of the fast-twitching muscles during the progression of the disease (like pSNAP-25S187 upregulation, which is normal in slow WT muscles). However, other molecular changes such as elevated pMunc18-1 and pSNAP-25 (T138) may represent an adaptative effort to ameliorate the increasing impairment of the neuromuscular function.

The precocious and sustained increase of TrkB.T1 along with the decrease of the functional receptor TrkB.FI, and the unbalance of pcPKC β I and pnPKC ϵ , seems to be specific of the ALS physiopathology and may be involved in the initial course of the disease. These molecular changes may deregulate the presynaptic function and decrease the retrograde neurotrophic protection over MNs. In the present study, we have not investigated morphologic changes in NMJ and axons. However, in accordance with our observation of precocious and sustained molecular changes in the BDNF-NT4/TrkB-p75/PKC-PKA/SNARE-SM pathway, a recent paper [88] shows that individual motoneurons in the slow disease progression SOD1-G37R mice model, synapses are gradually lost in a dynamic way (nerve terminal sprouting and

degeneration) at the tibialis anterior before the motoneurons completely degenerate suggesting the involvement of neuromuscular factors extrinsic to motor neurons. These data strongly point to a temporal window that could be therapeutically used in ALS. We hypothesize that the improvement of local signals from the neuromuscular environment (i.e. BDNF-NT4/TrkB signaling optimized by imposed physical training) could be key to maintain or prolong the synapse healthy and, thus, affect positively the motoneurons.

Acknowledgements This work has been possible with the financial support of Ministerio de Economía, Industria y Competitividad, the Agencia Estatal de Investigación (AEI) and the European Regional Development Fund (ERDF) (SAF2015-67143-P; PGC2018-097347-B-I00 grant submitted), the support of the Universitat Rovira i Virgili (URV) (2014PFR-URV-B2-83 and 2017PFR-URV-B2-85) and the Catalan Government (2014SGR344 and 2017SGR704). V.C. has been supported by the Ministerio de Economía y Competitividad (MINECO) under the framework of the Sistema Nacional de Garantía Juvenil, the European Social Fund (ESF) and the Iniciativa de Empleo Juvenil (IEJ).

Authors' Contributions LJ, EH, VC, MT: LJ, EH. LJ is responsible for data collection. LJ, EH, VC, OB, FC, JT, MAL, and NG are responsible for data interpretation. LJ, EH, VC, JT, MAL, and NG are responsible for literature search. LJ, EH, VC, JT, MAL, NG. JT, MAL, and NG are responsible for conception and design. All authors read and approved the final manuscript.

Compliance with Ethical Standards

Competing Interests The authors declare that they have no conflict of interest.

Ethics Approval and Consent to Participate The mice were cared for in accordance with the guidelines of the European Community's Council Directive of 24 November 1986 (86/609/EEC) for the humane treatment of laboratory animals. All experiments on animals have been reviewed and approved by the Animal Research Committee of the Universitat Rovira i Virgili (Reference number: 0233). Also, animal handling and experimentation were performed in line with approved Institutional Animal Care and Use Committee protocols at the University of Paris Descartes and followed the national authority (Ministère de la Recherche et de la Technologie, France) guidelines for the detention, use and the ethical treatment of laboratory animals based on European Union Directive 2010/63/EU.

Abbreviations ALS, Amyotrophic lateral sclerosis; BDNF, Brain derived neurotrophic factor; MN, Motoneuron; NMJ, Neuromuscular junction; NT4, Neurotrophin-4; p75^{NTR}, p75 neurotrophin receptor; PDK1, Phosphoinositide-dependent kinase-1; PKA, Protein kinase A; PKC, Protein kinase C; PLC γ , Gamma phospholipase C; SM, Sec1/Munc18-like; SNAP-25, Synaptosomal-associated protein 25; SNARE, Soluble NSF Attachment Protein (SNAP) receptor; TrkB, Tropomyosin-related kinase B receptor; WT, Wild type

References

- Kiernan MC, Vucic S, Cheah BC et al (2011) Amyotrophic lateral sclerosis. *Lancet* 377:942–955. [https://doi.org/10.1016/S0140-6736\(10\)61156-7](https://doi.org/10.1016/S0140-6736(10)61156-7)
- NIH NI of ND and S (2017) Amyotrophic lateral sclerosis, pp. 1–24
- Boillée S, Vande-Velde C, Cleveland DW (2006) ALS: a disease of motor neurons and their nonneuronal neighbors. *Neuron* 52:39–59. <https://doi.org/10.1016/j.neuron.2006.09.018>
- Pratt AJ, Getzoff ED, Perry JJP (2012) Amyotrophic lateral sclerosis: update and new developments. *Degener Neurol Neuromuscul Dis* 2012:1–14. <https://doi.org/10.2147/DNND.S19803>
- Rosen DR, Siddique T, Patterson D et al (1993) Mutations in Cu/Zn superoxide dismutase gene are associated with familial amyotrophic lateral sclerosis. *Nature* 362:59–62. <https://doi.org/10.1038/362059a0>
- Zheng C, Nennesmo I, Fadeel B, Henter J-I (2004) Vascular endothelial growth factor prolongs survival in a transgenic mouse model of ALS. *Ann Neurol* 56:564–567. <https://doi.org/10.1002/ana.20223>
- Moloney EB, de Winter F, Verhaagen J, et al (2014) ALS as a distal axonopathy: molecular mechanisms affecting neuromuscular junction stability in the presymptomatic stages of the disease. 8:1–18. <https://doi.org/10.3389/fmins.2014.00252>
- Fischer LR, Culver DG, Tennant P et al (2004) Amyotrophic lateral sclerosis is a distal axonopathy: evidence in mice and man. *Exp Neurol* 185:232–240. <https://doi.org/10.1016/j.expneurol.2003.10.004>
- Cleveland DW, Williamson TL (1999) Slowing of axonal transport is a very early event in the toxicity of ALS-linked SOD1 mutants to motor neurons. *Nat Neurosci* 2:50–56. <https://doi.org/10.1038/4553>
- Zhang B, Tu P, Abtahian F et al (1997) Neurofilaments and orthograde transport are reduced in ventral root axons of transgenic mice that express human SOD1 with a G93A mutation. *J Cell Biol* 139:1307–1315
- Lu B (2003) BDNF and activity-dependent synaptic modulation. *Learn Mem* 10:86–98
- Nadal L, Garcia N, Hurtado E et al (2017) Presynaptic muscarinic acetylcholine receptors and TrkB receptor cooperate in the elimination of redundant motor nerve terminals during development. *Front Aging Neurosci* 9:1–7. <https://doi.org/10.3389/fnagi.2017.00024>
- Nadal L, Garcia N, Hurtado E et al (2016) Presynaptic muscarinic acetylcholine autoreceptors (M1, M2 and M4 subtypes), adenosine receptors (A1 and A2A) and tropomyosin-related kinase B receptor (TrkB) modulate the developmental synapse elimination process at the neuromuscular junction. *Mol Brain* 9:1–19. <https://doi.org/10.1186/s13041-016-0248-9>
- Hurtado E, Cilleros V, Nadal L et al (2017) Muscle contraction regulates BDNF/TrkB signaling to modulate synaptic function through presynaptic cPKC α and cPKC β . *Front Mol Neurosci* 10:1–22. <https://doi.org/10.3389/fnmol.2017.00147>
- Mantilla CB, Stowe JM, Sieck DC et al (2014) TrkB kinase activity maintains synaptic function and structural integrity at adult neuromuscular junctions. *J Appl Physiol* 117:910–920. <https://doi.org/10.1152/jappphysiol.01386.2013>
- Ikeda K, Klinkosz B, Greene T et al (1995) Effects of brain-derived neurotrophic factor on motor dysfunction in wobbler mouse motor neuron disease. *Ann Neurol* 37:505–511. <https://doi.org/10.1093/jnen/61.2.142>
- Ikeda O, Murakami M, Ino H et al (2002) Effects of brain-derived neurotrophic factor (BDNF) on compression-induced spinal cord injury: BDNF attenuates down-regulation of superoxide dismutase expression and promotes up-regulation of myelin basic protein expression. *J Neuropathol Exp Neurol* 61:142–153
- Kobayashi E, Nakano H, Morimoto M, Tamaoki T (1989) Calphostin C (UCN-1028C), a novel microbial compound, is a highly potent and specific inhibitor of protein kinase C. *Biochem Biophys Res Commun* 159:548–553. [https://doi.org/10.1016/0006-291X\(89\)90028-4](https://doi.org/10.1016/0006-291X(89)90028-4)
- Haase G, Kennel P, Pettmann B et al (1997) Gene therapy of murine motor neuron disease using adenoviral vectors for neurotrophic factors. *Nat Med* 3:429–436
- Turner BJ, Cheah IK, Macfarlane KJ et al (2003) Antisense peptide nucleic acid-mediated knockdown of the p75 neurotrophin receptor

- delays motor neuron disease in mutant SOD1 transgenic mice. *J Neurochem* 87:752–763. <https://doi.org/10.1046/j.1471-4159.2003.02053.x>
21. Zhai J, Zhou W, Li J et al (2011) The in vivo contribution of motor neuron TrkB receptors to mutant SOD1 motor neuron disease. *Hum Mol Genet* 20:4116–4131. <https://doi.org/10.1093/hmg/ddr335>
 22. Yanpallear SU, Barrick CA, Buckley H et al (2012) Deletion of the BDNF truncated receptor TrkB.T1 delays disease onset in a mouse model of amyotrophic lateral sclerosis. *PLoS One* 7:1–7. <https://doi.org/10.1371/journal.pone.0039946>
 23. Mutoh T, Sobue G, Hamano T et al (2000) Decreased phosphorylation levels of TrkB Neurotrophin receptor in the spinal cords from patients with amyotrophic lateral sclerosis. *Neurochem Res* 25: 239–245. <https://doi.org/10.1023/A:1007575504321>
 24. Corse AM, Bilak MM, Bilak SR et al (1999) Preclinical testing of neuroprotective neurotrophic factors in a model of chronic motor neuron degeneration. *Neurobiol Dis* 6:335–346. <https://doi.org/10.1006/nbdi.1999.0253>
 25. Nagahara AH, Tuszynski MH (2011) Potential therapeutic uses of BDNF in neurological and psychiatric disorders. *Nat Rev Drug Discov* 10:209–219. <https://doi.org/10.1038/nrd3366>
 26. Gould TW, Oppenheim RW (2011) Motor neuron trophic factors: therapeutic use in ALS? *Brain Res Rev* 67:1–39. <https://doi.org/10.1016/j.brainresrev.2010.10.003>
 27. Nishio T, Sunohara N, Furukawa S (1998) Neurotrophin switching in spinal motoneurons of amyotrophic lateral sclerosis. *Neuroreport* 9: 1661–1665
 28. Besalduch N, Tomàs M, Santafé MM et al (2010) Synaptic activity-related classical protein kinase C isoform localization in the adult rat neuromuscular synapse. *J Comp Neurol* 518:211–228. <https://doi.org/10.1002/cne.22220>
 29. Obis T, Besalduch N, Hurtado E et al (2015) The novel protein kinase C epsilon isoform at the adult neuromuscular synapse: location, regulation by synaptic activity-dependent muscle contraction through TrkB signaling and coupling to ACh release. *Mol Brain* 8: 1–16. <https://doi.org/10.1186/s13041-015-0098-x>
 30. Simó A, Just-Borràs L, Cilleros-Mañé V et al (2018) BDNF-TrkB signaling coupled to nPKC ϵ and cPKC β I modulate the phosphorylation of the Exocytotic protein Munc18-1 during synaptic activity at the neuromuscular junction. *Front Mol Neurosci* 11:207–227. <https://doi.org/10.3389/fnmol.2018.00207>
 31. Nijssen J, Comley LH, Hedlund E (2017) Motor neuron vulnerability and resistance in amyotrophic lateral sclerosis. *Acta Neuropathol* 132:1–23. <https://doi.org/10.1007/s00401-017-1708-8>
 32. Deforges S, Branchu J, Biondi O et al (2009) Motoneuron survival is promoted by specific exercise in a mouse model of amyotrophic lateral sclerosis. *J Physiol* 587:3561–3571. <https://doi.org/10.1113/jphysiol.2009.169748>
 33. Hegedus J, Putman CT, Tyreman N, Gordon T (2008) Preferential motor unit loss in the SOD1 G93A transgenic mouse model of amyotrophic lateral sclerosis. *J Physiol* 586:3337–3351. <https://doi.org/10.1113/jphysiol.2007.149286>
 34. Marchetto MCN, Muotri AR, Mu Y, Smith AM, Cezar GG, Gage FH (2008) Non-cell-autonomous effect of human SOD1G37R astrocytes on motor neurons derived from human embryonic stem cells. *Cell Stem Cell* 3:649–657. <https://doi.org/10.1016/j.stem.2008.10.001>
 35. Tjust AE, Brannstrom T, Pedrosa Domellof F (2012) Unaffected motor endplate occupancy in eye muscles of ALS G93A mouse model. *Front Biosci (Schol Ed)* 4:1547–1555
 36. Harandi VM, Gaied ARN, Brännström T et al (2016) Unchanged neurotrophic factors and their receptors correlate with sparing in extraocular muscles in amyotrophic lateral sclerosis. *Investig Ophthalmology Vis Sci* 57:6831–6842. <https://doi.org/10.1167/iops.16-20074>
 37. Gurney ME, Pu H, Chiu AY et al (1994) Motor neuron degeneration in mice that express a human Cu,Zn superoxide dismutase mutation. *Science* (80-) 264:1772–1775
 38. Tu PH, Raju P, Robinson KA et al (1996) Transgenic mice carrying a human mutant superoxide dismutase transgene develop neuronal cytoskeletal pathology resembling human amyotrophic lateral sclerosis lesions. *Proc Natl Acad Sci U S A* 93:315531–315560
 39. McCombe PA, Henderson RD (2010) Effects of gender in amyotrophic lateral sclerosis. *Gend Med* 7:557–570. <https://doi.org/10.1016/j.genm.2010.11.010>
 40. Obis T, Hurtado E, Nadal L et al (2015) The novel protein kinase C epsilon isoform modulates acetylcholine release in the rat neuromuscular junction. *Mol Brain* 8:1–16. <https://doi.org/10.1186/s13041-015-0171-5>
 41. Hurtado E, Cilleros V, Just L et al (2017) Synaptic activity and muscle contraction increases PDK1 and PKC β I phosphorylation in the presynaptic membrane of the neuromuscular junction. *Front Mol Neurosci* 10:1–13. <https://doi.org/10.3389/fnmol.2017.00270>
 42. Aldridge GM, Podrebarac DM, Greenough WT, Weiler IJ (2008) The use of total protein stains as loading controls: An alternative to high-abundance single-protein controls in semi-quantitative immunoblotting. *J Neurosci Methods* 172:250–254. <https://doi.org/10.1016/j.jneumeth.2008.05.003>
 43. Zheng Z, Sabirzhanov B, Keifer J (2010) Oligomeric amyloid-inhibits the proteolytic conversion of brain-derived neurotrophic factor (BDNF), AMPA receptor trafficking, and classical conditioning. *J Biol Chem* 285:34708–34717. <https://doi.org/10.1074/jbc.M110.150821>
 44. Middlemas DS, Meisenhelder J, Hunter T (1994) Identification of TrkB autophosphorylation sites and evidence that phospholipase C-gamma1 is a substrate of the TrkB receptor. *J Biol Chem* 269:5458–5466
 45. Eide FF, Vining ER, Eide BL et al (1996) Naturally occurring truncated trkB receptors have dominant inhibitory effects on brain-derived neurotrophic factor signaling. *J Neurosci* 16:3123–3129. <https://doi.org/10.1523/JNEUROSCI.16-10-03123.1996>
 46. Santafé MM, Garcia N, Tomàs M et al (2014) The interaction between tropomyosin-related kinase B receptors and serine kinases modulates acetylcholine release in adult neuromuscular junctions. *Neurosci Lett* 561:171–175. <https://doi.org/10.1016/j.neulet.2013.12.073>
 47. Song W, Jin XA (2015) Brain-derived neurotrophic factor inhibits neuromuscular junction maturation in a cAMP-PKA-dependent way. *Neurosci Lett* 591:8–12. <https://doi.org/10.1016/j.neulet.2015.02.019>
 48. Dulubova I, Sugita S, Hill S et al (1999) A conformational switch in syntaxin during exocytosis: role of munc18. *EMBO J* 18:4372–4382. <https://doi.org/10.1093/emboj/18.16.4372>
 49. Misura KM, Scheller RH, Weis WI (2000) Three-dimensional structure of the neuronal-Sec1-syntaxin 1a complex. *Nature* 404: 355–362. <https://doi.org/10.1038/35006120>
 50. Verhage M, Maia AS, Plomp JJ et al (2000) Synaptic assembly of the brain in the absence of neurotransmitter secretion. *Science* 287: 864–869. <https://doi.org/10.1126/science.287.5454.864>
 51. Yang B, Steegmaier M, Gonzalez LC, Scheller RH (2000) nSec1 binds a closed conformation of syntaxin1A. *J Cell Biol* 148:247–252
 52. Liu J, Ernst SA, Gladychyeva SE et al (2004) Fluorescence resonance energy transfer reports properties of syntaxin1a interaction with Munc18-1 in vivo. *J Biol Chem* 279:55924–55936. <https://doi.org/10.1074/jbc.M410024200>
 53. Hata Y, Slaughter CA, Südhof TC (1993) Synaptic vesicle fusion complex contains unc-18 homologue bound to syntaxin. *Nature* 366:347–351. <https://doi.org/10.1038/366347a0>
 54. Medine CN, Rickman C, Chamberlain LH, Duncan RR (2007) Munc18-1 prevents the formation of ectopic SNARE complexes

- in living cells. *J Cell Sci* 120:4407–4415. <https://doi.org/10.1242/jcs.020230>
55. de Vries KJ, Geijtenbeek A, Brian EC et al (2000) Dynamics of munc18-1 phosphorylation/dephosphorylation in rat brain nerve terminals. *Eur J Neurosci* 12:385–390. <https://doi.org/10.1046/j.1460-9568.2000.00931.x>
 56. Dulubova I, Khvotchev M, Liu S et al (2007) Munc18-1 binds directly to the neuronal SNARE complex. *Proc Natl Acad Sci U S A* 104:2697–2702. <https://doi.org/10.1073/pnas.0611318104>
 57. Fujita Y, Sasaki T, Fukui K et al (1996) Phosphorylation of Munc-18/n-Sec1/rbSec1 by protein kinase C: Its implication in regulating the interaction of Munc-18/n-Sec1/rbSec1 with syntaxin. *J Biol Chem* 271:7265–7268
 58. Genc O, Kochubey O, Toonen RF et al (2014) Munc18-1 is a dynamically regulated PKC target during short-term enhancement of transmitter release. *Elife* 3:1715–1734. <https://doi.org/10.7554/eLife.01715>
 59. Südhof TC, Rothman JE (2009) Membrane fusion: grappling with SNARE and SM proteins. *Science* 323:474–477. <https://doi.org/10.1126/science.1161748>
 60. Leenders AGM, Sheng Z-H (2005) Modulation of neurotransmitter release by the second messenger-activated protein kinases: implications for presynaptic plasticity. *Pharmacol Ther* 105:69–84. <https://doi.org/10.1016/j.pharmthera.2004.10.012>
 61. Nagy G, Matti U, Nehring RB et al (2002) Protein kinase C-dependent phosphorylation of synaptosome-associated protein of 25 kDa at Ser187 potentiates vesicle recruitment. *J Neurosci* 22:9278–9286. <https://doi.org/10.1523/JNEUROSCI.22-21-09278.2002>
 62. Dorsey SG, Lovering RM, Renn CL et al (2011) Genetic deletion of *trkB.T1* increases neuromuscular function. *Am J Physiol - Cell Physiol* 302:141–153. <https://doi.org/10.1152/ajpcell.00469.2010>
 63. Küst BM, Copray JCV, Brouwer N et al (2002) Elevated levels of Neurotrophins in human biceps Brachii tissue of amyotrophic lateral sclerosis. *Exp Neurol* 177:419–427. <https://doi.org/10.1006/exnr.2002.8011>
 64. Hempstead BL (2002) The many faces of p75NTR. *Curr Opin Neurobiol* 12:260–267. [https://doi.org/10.1016/S0959-4388\(02\)00321-5](https://doi.org/10.1016/S0959-4388(02)00321-5)
 65. Peng HB, Yang J-F, Dai Z et al (2003) Differential effects of neurotrophins and schwann cell-derived signals on neuronal survival/growth and synaptogenesis. *J Neurosci* 23:5050–5060. <https://doi.org/10.1523/JNEUROSCI.23-12-05050.2003>
 66. Mantilla CB, Gransee HM, Zhan W-Z, Sieck GC (2013) Motoneuron BDNF/TrkB signaling enhances functional recovery after cervical spinal cord injury. *Exp Neurol* 247:101–109. <https://doi.org/10.1016/j.expneurol.2013.04.002>
 67. Ochs G, Penn RD, York M et al (2000) A phase I/II trial of recombinant methionyl human brain derived neurotrophic factor administered by intrathecal infusion to patients with amyotrophic lateral sclerosis. *Amyotroph Lateral Scler Other Motor Neuron Disord* 1: 201–206
 68. Beck M, Flachenecker P, Magnus T et al (2005) Autonomic dysfunction in ALS: a preliminary study on the effects of intrathecal BDNF. *Amyotroph Lateral Scler Other Motor Neuron Disord* 6: 100–103. <https://doi.org/10.1080/14660820510028412>
 69. Patapoutian A, Reichardt LF (2001) Trk receptors: mediators of neurotrophin action. *Curr Opin Neurobiol* 11:272–280. [https://doi.org/10.1016/S0959-4388\(00\)00208-7](https://doi.org/10.1016/S0959-4388(00)00208-7)
 70. Garcia N, Priego M, Obis T et al (2013) Adenosine A1 and A2A receptor-mediated modulation of acetylcholine release in the mice neuromuscular junction. *Eur J Neurosci* 38:2229–2241. <https://doi.org/10.1111/ejn.12220>
 71. Tomàs J, Garcia N, Lanuza MA et al (2017) Presynaptic membrane receptors modulate ACh release, axonal competition and synapse elimination during neuromuscular junction development. *Front Mol Neurosci* 10:1–12. <https://doi.org/10.3389/FNMOL.2017.00132>
 72. Felipe V, Miñana MD, Grisolia S (1993) Inhibitors of protein kinase C prevent the toxicity of glutamate in primary neuronal cultures. *Brain Res* 604:192–196. [https://doi.org/10.1016/0006-8993\(93\)90368-W](https://doi.org/10.1016/0006-8993(93)90368-W)
 73. Krieger C, R a L, Pelech SL, C a S (1996) Amyotrophic lateral sclerosis: the involvement of intracellular Ca²⁺ and protein kinase C. *Trends Pharmacol Sci* 17:114–120. [https://doi.org/10.1016/0165-6147\(96\)10004-3](https://doi.org/10.1016/0165-6147(96)10004-3)
 74. Mondola P, Damiano S, Sasso A, Santillo M (2016) The Cu, Zn superoxide dismutase: not only a dismutase enzyme. *Front Physiol* 7:1–8. <https://doi.org/10.3389/fphys.2016.00594>
 75. Nagao M, Kato S, Oda M, Hirai S (1998) Decrease of protein kinase C in the spinal motor neurons of amyotrophic lateral sclerosis. *Acta Neuropathol* 96:52–56. <https://doi.org/10.1007/s004010050859>
 76. Amieux PS, Cummings DE, Motamed K et al (1997) Compensatory regulation of R1alpha protein levels in protein kinase a mutant mice. *J Biol Chem* 272:3993–3998
 77. Brandon EP, Idzerda RL, McKnight GS (1997) PKA isoforms, neural pathways, and behaviour: making the connection. *Curr Opin Neurobiol* 7:397–403. [https://doi.org/10.1016/S0959-4388\(97\)80069-4](https://doi.org/10.1016/S0959-4388(97)80069-4)
 78. Hu J-H, Zhang H, Wagey R et al (2003) Protein kinase and protein phosphatase expression in amyotrophic lateral sclerosis spinal cord. *J Neurochem* 85:432–442. <https://doi.org/10.1046/j.1471-4159.2003.01670.x>
 79. Hu JH, Chernoff K, Pelech S, Krieger C (2003) Protein kinase and protein phosphatase expression in the central nervous system of G93A mSOD over-expressing mice. *J Neurochem* 85:422–431. <https://doi.org/10.1046/j.1471-4159.2003.01669.x>
 80. Plomp JJ, Vergouwe MN, Van den Maagdenberg AM et al (2000) Abnormal transmitter release at neuromuscular junctions of mice carrying the tottering alpha1A Ca²⁺ channel mutation. *Brain* 123: 463–471. <https://doi.org/10.1093/brain/123.3.463>
 81. Eisen A (2001) Clinical electrophysiology of the upper and lower motor neuron in amyotrophic lateral sclerosis. *Semin Neurol* 21: 141–154. <https://doi.org/10.1055/s-2001-15261>
 82. Rocha MC, Pousinha PA, Correia AM et al (2013) Early changes of neuromuscular transmission in the SOD1(G93A) mice model of ALS start long before motor symptoms onset. *PLoS One* 8:1–11. <https://doi.org/10.1371/journal.pone.0073846>
 83. Wood SJ, Slater CR (1997) The contribution of postsynaptic folds to the safety factor for neuromuscular transmission in rat fast- and slow-twitch muscles. *J Physiol* 500:165–176
 84. Dupuis L, Pradat P-F, Ludolph AC, Loeffler J-P (2011) Energy metabolism in amyotrophic lateral sclerosis. *Lancet Neurol* 10: 75–82. [https://doi.org/10.1016/S1474-4422\(10\)70224-6](https://doi.org/10.1016/S1474-4422(10)70224-6)
 85. Dupuis L, Gonzalez De Aguilar JL, Oudart H et al (2004) Mitochondria in amyotrophic lateral sclerosis: a trigger and a target. *Neurodegener Dis* 1:245–254. <https://doi.org/10.1159/000085063>
 86. Palamiuc L, Schlagowski A, Ngo ST et al (2015) A metabolic switch toward lipid use in glycolytic muscle is an early pathologic event in a mouse model of amyotrophic lateral sclerosis. *EMBO Mol Med* 7:526–546. <https://doi.org/10.15252/emmm.201404433>
 87. Gertler RA, Robbins N (1978) Differences in neuromuscular transmission in red and white muscles. *Brain Res* 142:160–164. [https://doi.org/10.1016/0006-8993\(78\)90186-5](https://doi.org/10.1016/0006-8993(78)90186-5)
 88. Martineau É, Di Polo A, Vande Velde C, Robitaille R (2018) Dynamic neuromuscular remodeling precedes motor-unit loss in a mouse model of ALS. *Elife* 7:1–19. <https://doi.org/10.7554/eLife.41973>